Path Planning for UAV-Ship Collaborative Search and Rescue Considering Ship Dynamics

Rongjie Tang
School of Navigation, Dalian Maritime University, Dalian, Liaoning, China

Abstract: To address the challenge posed by the dynamic movement of the mother ship to the safety of UAV return-to-base operations during maritime search and rescue, this study proposes a UAV-ship collaborative search and rescue path planning method that incorporates ship motion prediction. At the modeling level, a collaborative search model was constructed that integrates gridded sea areas, target probability updates, anisotropic wind resistance energy consumption, and ship dynamic takeoff and landing window constraints.At the algorithmic level, an Improved Coati Optimization Algorithm(ICOA) was designed, integrating dynamic adversarial learning initialization and covariance matrix guidance, and incorporating an exponential penalty function mechanism based on safety margins. Simulation results show that in static scenarios, PSO performs best (detection probability 0.0283), while ICOA ranks in the middle;in dynamic scenarios, the proposed method improves the safety margin from -470.02 to -0.13 ($p < 0.001$), whereas the scheme that does not account for vessel movement results in 30 crashes into the sea. Ablation experiments validate the independent contributions of each improvement. The proposed method demonstrates significant advantages in both search and rescue effectiveness and flight safety.

Keywords: Maritime Search and Rescue; UAV Path Planning; IMPROVED Coati Optimization Algorithm; Dynamic Return-to-home Constraint

1. Introduction

1.1 Research Background and Significance

Maritime transport accounts for approximately 90% of international trade volume and serves as the lifeblood of global commerce. According to Allianz Commercial's *2025 Safety and Shipping Report*, there were 3,310 global shipping accidents in 2024, a 10% year-over-year increase and a ten-year high. The demand for routine, high-efficiency maritime search and rescue operations is becoming increasingly urgent.

Quadcopter UAVs, with their compact size, vertical takeoff and landing capabilities, and high maneuverability, can be deployed directly from a ship's deck. Compared to fixed-wing UAVs, they possess the ability to hover at a fixed point; compared to manned helicopters, they offer lower operational costs and eliminate the risk of human casualties.Messmer et al. [1] and Wen et al. [2] have pointed out that UAVs are highly suited for maritime search missions, and proper path planning can significantly enhance search and rescue efficiency. However, relying solely on UAVs presents bottlenecks such as limited endurance. The "mother-ship–daughter-UAV" collaborative model, which uses a ship as a mobile takeoff and landing platform and UAVs as sensing nodes, can greatly expand operational capabilities.

Existing research has made progress in areas such as multi-UAV collaborative coverage [3,9], optimization under adverse weather conditions [4], and target drift modeling [4], but shortcomings remain: first, most studies treat the vessel as a fixed takeoff and landing point, neglecting the hard constraint of the mother ship's dynamic displacement on the return flight; second, standard swarm intelligence algorithms are prone to premature convergence in wide-area sparse search spaces.Therefore, developing path planning algorithms that integrate vessel dynamics into the optimization framework holds significant theoretical and engineering value.

1.2 Current State of Domestic and International Research

Ship search and rescue path planning: Du Yonghao et al. [5] established a multi-platform collaborative search path optimization model and designed a distributed optimization strategy.Luo Xiubo et al. [6] proposed a dual-lifeboat search and rescue strategy based on the ant colony algorithm. Akbari et al. [7] proposed a multi-objective optimization model for the allocation of search and rescue vessel positions. Wang Haoliang et al. [3] studied collaborative path tracking control for UAV-USV swarms, providing low-level control support for the “mother ship–subordinate aircraft” mode.

UAV Search and Rescue Path Planning: Cho et al. [9-10] proposed a coverage path planning method based on hexagonal grid decomposition. Ma et al. [4] proposed an improved multi-task optimization method using NSGA-II.Zhang Wenjun et al. [11] introduced a Gaussian mixture model to guide multi-UAV search. Sun et al. [8] combined an improved ant colony algorithm with YOLOv8 to achieve collaborative planning and intelligent perception. Wen et al. [2] were the first to incorporate target mobility into the path planning framework.

Review of the Current State: Existing research has made significant progress in collaborative search frameworks, coverage path planning, and the application of swarm intelligence algorithms. However, two issues remain: the lack of dynamic vessel constraints and insufficient algorithmic adaptability. This paper proposes treating the dynamic position of the vessel as a hard constraint and designs an ICOA algorithm that integrates dynamic adversarial learning with covariance guidance to enhance search and rescue efficiency and return-to-port safety under complex sea conditions.

1.3 Research Content and Technical Approach

(1) Modeling of Maritime SAR Scenarios: Sea area gridding, wind field energy consumption, target probability distribution, and vessel dynamic models.

(2) ICOA Algorithm Design: Initialization via dynamic adversarial learning, covariance matrix guidance, and constraint handling using a dual-fitness penalty function.

(3) UAV-Vessel Coordination Mechanism: Dynamic takeoff and landing window constraints, return-to-base safety margin assessment.

(4) Simulation Experiments: Five sets of progressive comparative experiments to validate algorithm performance and the necessity of constraints.

1.3.1 Research scope

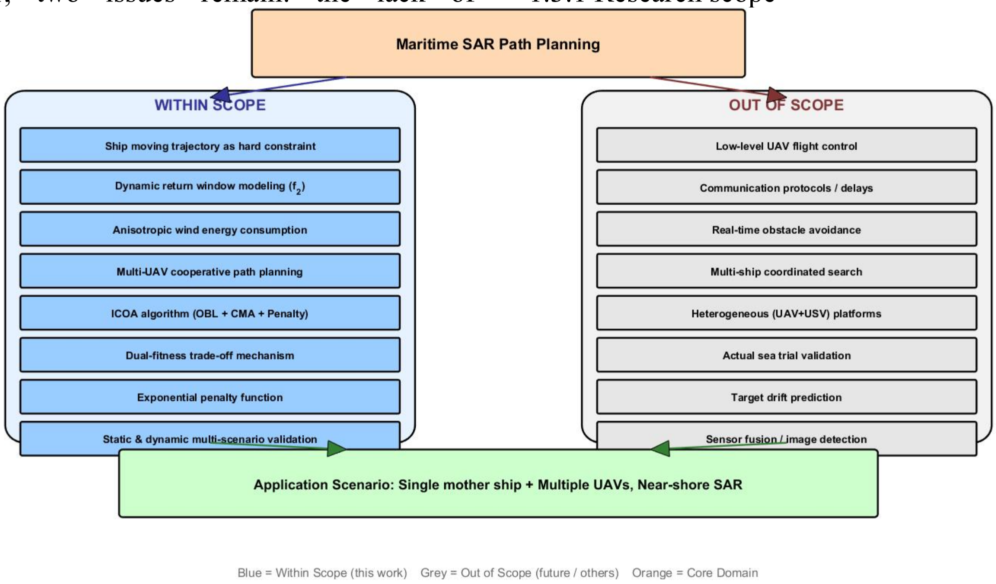

Figure 1. Research Scope of the UAV-ship Collaborative Search and Rescue System

As illustrated in Fig. 1:

(1) Modeling of Maritime Search and Rescue Scenarios

Establish a 3D maritime search and rescue environment model, primarily including:

Marine topography and no-fly zones; wind field models; target location probability distributions; vessel dynamic models.

(2) Design of Multi-Drone Cooperative Path Planning Algorithms

Design path planning strategies based on improved swarm intelligence algorithms:

1) Selection of the base algorithm; 2) Algorithm improvements; 3) Multi-drone coordination mechanisms; 4. Constraint handling.

(3) Research on UAV-Vessel Coordination

Mechanisms

Research on dynamic coordination methods between UAVs and vessels:

Dynamic takeoff and landing point planning; emergency return-to-base strategies; utilization of communication relays;

(4) Simulation Experiments and Performance Evaluation

Develop a MATLAB simulation platform and design comparative experiments:

1) Comparing search efficiency with standard search modes (parallel search, expanded square);

2) Comparison of convergence speed and path quality with classical algorithms (genetic algorithms, simulated annealing);

3) Robustness testing under different sea conditions;

4) Analysis of multi-machine collaboration effects;

1.3.2 Technical approach

As illustrated in Fig. 2

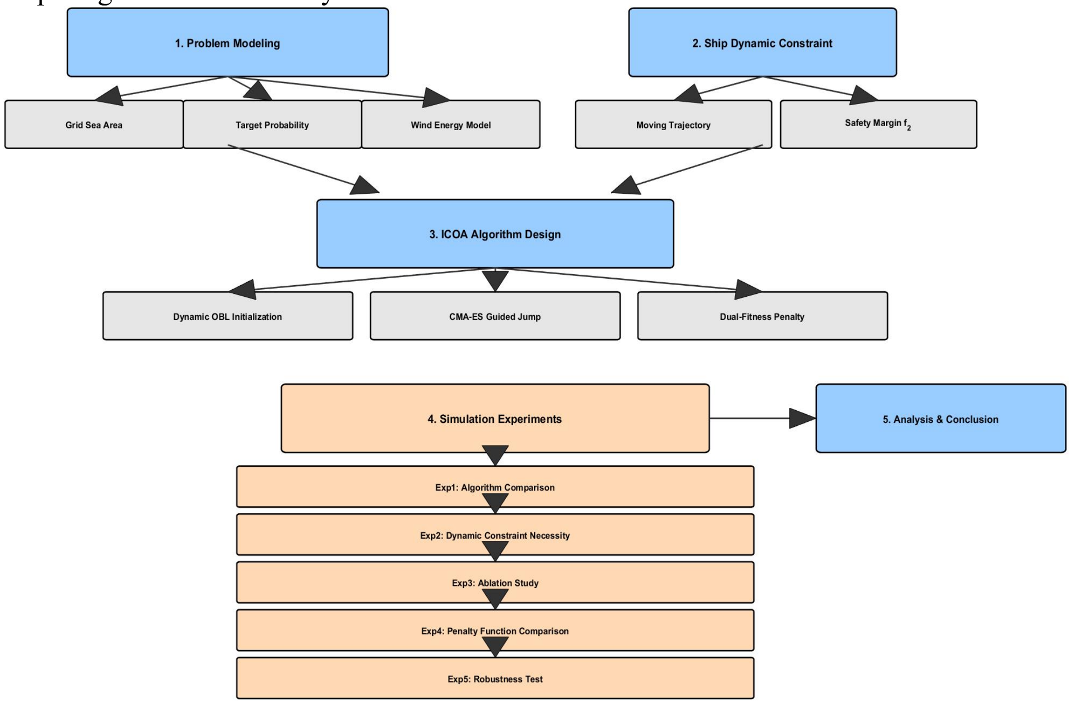

Figure 2. Technical Approach Flowchart

2. Problem Modeling and Algorithm Design

2.1 Search and Rescue Scenario and Maritime Grid Division

The search and rescue system consists of a moving mother ship and M quadcopter UAVs. The mother ship continuously moves through wind and waves, serving as a mobile takeoff and landing platform for the UAVs. The sea area is discretized into a G×G uniform grid (with side length L), where the grid cell size is L/G.At each step, a UAV moves to an adjacent grid cell or hovers; direction codes {1, 2, …, 8} correspond to the eight-neighborhood, and 9 denotes hovering. The path of a single UAV is encoded as a sequence of actions $a_t \in \{1, \ldots, 9\}$ of length T, while the coordinated path of multiple UAVs is encoded as the concatenation of individual paths, with a total dimension of M × T.

2.2 Target Presence Probability Model

The initial probability of target presence follows a trinomial Gaussian mixture distribution. During the search, when a UAV visits a grid cell, the probability of that cell is updated using Bayes' rule: if no target is detected, the probability is multiplied by the miss rate p_{miss} and then normalized across the entire map. The cumulative detection probability f_1 is defined as the sum of the detection probability increments at each step along the path:

$$f_1=\sum_{t=1}^{T} P\,(i_t,j_t)\cdot(1-p_{miss}) \qquad (1)$$

2.3 Anisotropic Wind Resistance Energy Consumption Model

The UAV experiences varying wind resistance depending on its heading.The required airspeed v_a is calculated as the square root of the difference between ground speed v_g and wind speed v_w ($v_a = \|v_g - v_w\|$), and energy consumption is proportional to v_a². Energy consumption values $\{e_1, \ldots, e_9\}$ are precomputed for eight directions and hovering, and the remaining battery capacity at each step is $E_{t+1} = E_t - e_{a_t}$.

2.4 Constraints on the Ship's Dynamic Takeoff and Landing Window

Unlike previous studies that simplify the mother ship to a fixed takeoff/landing point, this paper treats its continuous motion as a hard constraint. The mother ship's trajectory adopts a composite model consisting of uniform linear motion superimposed with sinusoidal sway. The return-to-base safety margin f_2 is defined as the difference between the remaining battery charge and the estimated energy consumption for the return trip:

$$f_2 = E_{remain} - E_{return} \tag{2}$$

$f_2 \geq 0$ indicates a safe return, while $f_2 < 0$ indicates a risk of falling into the sea.

2.5 Collaborative Search Optimization Model

The path planning problem is formalized as a constrained optimization problem: maximize the search and rescue benefit f_1 while satisfying the return-to-base safety constraint $f_2 \geq 0$. An exponential penalty function is used to incorporate the constraint into the objective:

$$F = f_1 - P(\Delta E) \tag{3}$$

$$P(\Delta E) = \begin{cases} 0, & \Delta E \leq 0 \\ \lambda \cdot \left(e^{\mu \cdot \Delta E} - 1\right), & \Delta E > 0 \end{cases} \tag{4}$$

2.6 Improved Coati Optimization Algorithm (ICOA)

Improved Coati Optimization Algorithm[13] is a meta-heuristic algorithm that simulates the collective behavior of a group of ring-tailed coati. Its cooperative climbing mechanism during the foraging phase is suitable for wide-area space exploration, while its convergence-oriented aggregation mechanism during the escape phase facilitates local convergence. However, the original ICOA[13] uses purely random initialization, which causes the initial population to easily deviate from high-probability regions in sparse search spaces, and it lacks a mechanism to address stagnation. To address these issues, this paper introduces two improvements.

(1) Dynamic Oppositional Learning (DOBL)[14] Initialization:

In the initialization phase, this paper draws on the concept of adversarial learning to generate evaluation points at symmetric positions using an adaptive probability. After merging the original individuals with the adversarial individuals, the top N are selected based on fitness. This paper introduces an adaptive probability p_obl to regulate the proportion of adversarial solutions generated:

$$p_{obl} = 1 - \frac{1}{1 + \exp(-\sigma_f)} \tag{5}$$

where σ_f is the standard deviation of the initial population's fitness. After merging the original individuals with the opposing individuals, the top N are selected based on fitness, forming a high-quality initial population.

Opposite relationship in a two-dimensional space: (as illustrated in Fig. 3)

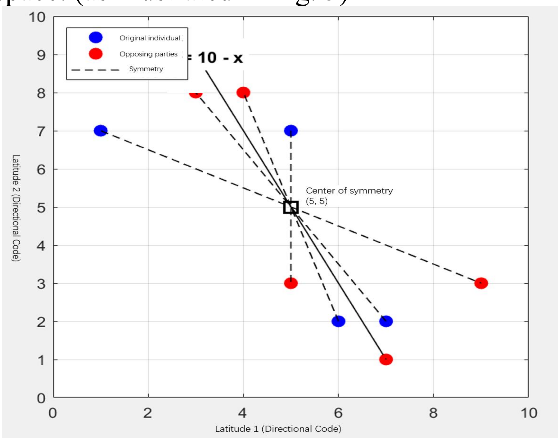

Figure 3. Schematic Diagram of Oppositional Relationship in Two-dimensional Space

Flowchart of the dynamic adversarial learning screening process: (as illustrated in Fig. 4)

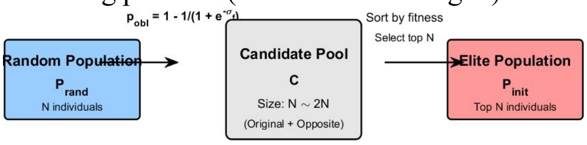

Figure 4. Flowchart of Dynamic Oppositional Learning Screening Process

(2) Covariance Matrix Adaptive Steering (CMA)

Drawing on CMA-ES [12], when the global optimum has not improved for τ consecutive iterations, a new individual is generated along the dominant direction using the covariance matrix of the elite subpopulation to replace the worst individual, thereby restoring search diversity.

(3) Dual-fitness exponential penalty function

f_2 is incorporated into the total fitness $F = f_1 - P(\Delta E)$ as an exponential penalty function, enabling the algorithm to automatically converge toward the safe return zone while optimizing search and rescue efficiency.

ICOA Flowchart as illustrated in Fig. 5

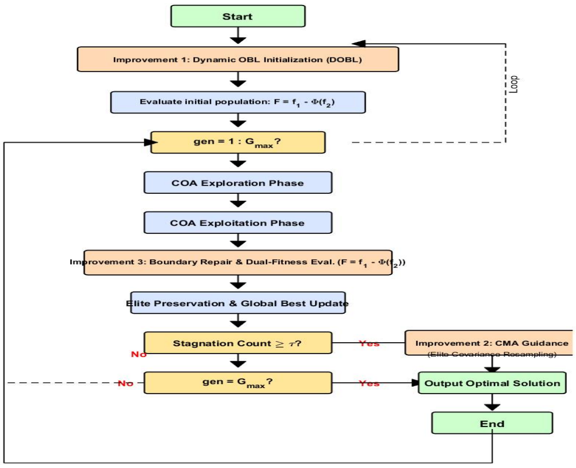

Figure 5. Flowchart of the ICOA Algorithm

3. Simulation Experiments and Analysis

To validate the effectiveness of the proposed ICOA algorithm and the dynamic vessel constraint mechanism, this chapter establishes a multi-scenario simulation platform in the MATLAB R2024b environment and designs five sets of progressive comparative experiments.This chapter first presents the simulation environment and parameter settings (Section 3.1), followed by a verification of the algorithm's optimization capability (Section 3.2), a verification of the necessity of dynamic vessel constraints (Section 3.3), ablation experiments on the improved strategy (Section 3.4), a comparison of constraint handling mechanisms (Section 3.5), and comprehensive robustness testing (Section 3.6). Finally, the chapter concludes with a summary and discussion of the experiments (Section 3.7).

3.1 Simulation Environment and Parameters

3.1.1 Basic scenario parameters, as shown in Table 1

Table 1. Basic Scenario Parameters

Parameters	Symbol	Value
Sea Area Boundary Length	L	9.6 km
Number of grid cells	-	96×96
Grid cell size	-	100 m
Maximum number of drone flights	T	192
Duration per step	△t	55 s
Number of drones	M	2
Initial drone battery level	E_0	100 m/s
Drone airspeed	v_air	15
Sensor false negative rate	p_miss	0.2
Target probability distribution	-	Trileve Gaussian mixture

3.1.2 Differentiated settings for each experiment, as shown in Table 2

Table 2. Differentiated Settings

Parameters	Experiment 1	Experiments 2/3/4	Experiment 5
Wind Speed at Sea Level	0 m/s	4 m/s (Force 5)	0/4/8 m/s
Mothership speed	0 knots (at rest)	7 kn	4/7/10 knots
Mothership behavior	Fixed takeoff and landing points	Straight course -90^0 + Sine yaw	Variable
Wind Field Energy Consumption	Isotropic	Isotropic	Anisotropic
Maximum number of iterations	300	200	200
Initial charge	100	400	350

3.1.3 Comparison of algorithms and parameters, as shown in Table 3

Table 3. Comparison of Algorithms and Parameters

Parameter	Value
Population Size N	40
Maximum Number of Iterations G_max	300 (Experiment 1)/200 (Experiments 2–5)
Probability of "learning from peers" during the exploration phase	0.5
Trigger probability during the development phase	0.3
Probability of "learning from the best" in the development phase (per dimension)	0.5
PSO inertia weight w	0.7
PSO learning factors c_1, c_2	1.5, 1.5
GA crossover probability	0.8

ICOA-specific parameters, as shown in Table 4

Table 4. ICOA-specific Parameters

Parameter Symbol	Parameter Meaning	Value
τ	Stagnation Threshold (CMA Trigger Condition)	10
γ	CMA replacement ratio	0.3
λ	Penalty Amplitude Coefficient	480 (dynamic scenes) / 100 (static scenes)
μ	Penalty exponential growth rate	2.1 (dynamic scenes) / 1.0 (static scenes)

3.1.4 Evaluation metrics, as shown in Table 4

Table 4. Evaluation Metrics

Metric	Definition	Meaning
Cumulative Detection Probability	Sum of Bayesian updated probabilities for path-covered grids	Search and Rescue Benefit
Coverage	Proportion of total grids	Spatial search

	visited	breadth
Return success rate	Number of missions successfully returning to the mobile mother ship / Total number of operations	Flight Safety
Safety margin f_2	Difference between remaining battery power and estimated energy consumption for return	Quantification of Return-to-Base Safety
Number of CMA triggers	Number of times covariance guidance is activated during the search process	Population diversity maintenance

3.2 Experiment 1: Evaluation of Algorithm Optimization Capabilities

3.2.1 Experiment Objectives and Setup

This experiment aims to eliminate complex factors such as ship movement and wind fields, and to purely compare the optimization capabilities of ICOA with mainstream algorithms and traditional search methods in a static sea environment.

Scenario setup: A 9.6 km × 9.6 km sea area with a 96 × 96 grid. The mother ship remains stationary at a fixed takeoff/landing point, and there is no wind field. Two UAVs are used, with a maximum number of steps of 192 and an initial battery charge of 100. The population size is N = 40, and the maximum number of iterations is G_max = 300. Each algorithm is run independently 30 times.

3.2.2 Experimental results, as shown in Table 5

Table 5. Results of Experimental 1

Algorithm	Cumulative Detection Probability (Mean + Standard Deviation)	Coverage (%)	Convergence Iterations (Mean)
ICOA	0.0210 ± 0.0033	1.20 ± 0.10	300*
COA	0.0218 ± 0.0024	1.25 ± 0.10	300*
PSO	0.0283 ± 0.0026	1.35 ± 0.07	300*
GA	0.0210 ± 0.0026	1.16 ± 0.11	300*

Data Plot for Experiment 1, as illustrated in Fig. 6

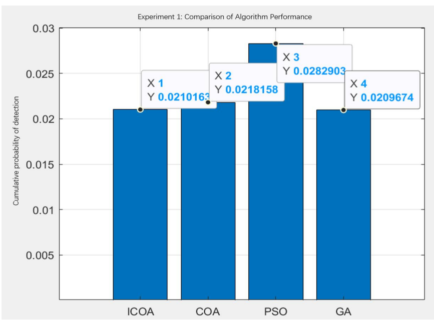

Figure 6. Convergence Curves and Detection Probability of Four Algorithms in Experiment 1

3.2.3 Analysis of Results

The cumulative discovery probabilities of the four algorithms are ranked as follows: PSO (0.0283) > COA (0.0218) ≈ ICOA (0.0210) ≈ GA (0.0210).It is worth noting that the original version of COA (0.0218) is slightly higher than the improved ICOA (0.0210), indicating that under unconstrained conditions, the additional exploration mechanism may slightly weaken the ability for fine-grained search. ICOA did not demonstrate an advantage in static scenarios because its improvement strategies (OBL, CMA) are designed for dynamic constraints; in flat spaces, it may instead sacrifice fine-grained search due to excessive exploration.None of the four algorithms converged within 300 iterations, indicating that this problem exhibits characteristics of large-scale discrete optimization.

3.3 Experiment 2: Verification of the Necessity of Dynamic Ship Constraints

3.3.1 Experiment Objectives and Setup

To verify the necessity of the ship's dynamic position as a hard constraint for the UAV's return-to-base, two sets of comparative experiments were conducted:

Scenario A (Dynamic Constraint): During ICOA optimization, the fitness function includes an exponential penalty term based on the mother ship's real-time trajectory, guiding the UAV to approach the moving mother ship in the latter stages of the mission.

Scheme B (Ignoring Movement): During ICOA optimization, the mother ship is assumed to be fixed at its initial position, but it actually moves during path execution to test its true return-to-base capability.

Scenario: A 9.6 km × 9.6 km sea area with a 96 × 96 grid. Wind speed: 5 m/s; wind direction: 45°. The mother ship moves southward from (1000, 8000) at a speed of 7 knots. The target probability distribution is a three-peak Gaussian mixture model centered in the middle of the sea area. Two UAVs are used, with an initial battery capacity of 400 and a maximum number of steps of 96.

Each scenario was run independently 30 times, recording the homing success rate, number of crashes into the sea, safety margin f_2, and cumulative detection probability. An independent samples t-test was performed on f_2.

3.3.2 Experimental results, as shown in Table 6.

Conclusion: The safety margin of Scheme A is significantly higher than that of Scheme B ($p < 0.000$), and dynamic constraints enhance return-to-base safety.

Table 6. Results of Experimental 2

Metrics	Scenario A (Constrained)	Scenario B (Unconstrained)
Return Success Rate	0.00%	0.00%
Number of crashes into the sea	30 / 30	30 / 30
Safety margin f2	-0.13 ± 0.17	-470.02 ± 49.33
Cumulative detection probability	0.0000 ± 0.0000	0.0001 ± 0.0001
t-test p-value (F2)	-	0.0000

3.3.3 Analysis of results

Scheme A has a safety margin of -0.13, requiring only minor battery adjustments for return; Scheme B has a safety margin of -470.02, a deficit 3,616 times that of Scheme A, representing an extremely significant difference ($p < 0.001$).The cumulative discovery probabilities for both groups are near zero. Under the penalty function, Scheme A prioritizes safety by sacrificing search coverage, while Scheme B conducts an exhaustive search but results in all 30 attempts ending in a crash into the sea. The above comparison validates the necessity of dynamic return-to-base constraints and the effectiveness of the exponential penalty function.

3.4 Experiment 3: Ablation Study of the Improved Strategy

3.4.1 Experiment Objectives and Setup

To quantify the independent contributions of the two improved strategies-dynamic Oppositional Learning Initialization (OBL) and Covariance Matrix Adaptive Guidance (CMA)-to ICOA performance, four algorithm configurations were set up for ablation comparison, as shown in Table 7.

Table 7. Ablation Comparison

Configuration	Dynamic Oppositional Learning	Covariance Guidance	Description
ICOA	✓	✓	Complete algorithm
ICOA-noOBL	✗	✓	Retain only CMA guidance; initialization changed to random
ICOA-noCMA	✓	✗	Retain only OBL initialization; no covariance guidance
COA	✗	✗	Original Tail-of-the-Distribution Algorithm

Scenario: Static sea area (no wind, stationary mother ship), 96×96 grid, maximum number of steps 192, target probability distribution as a trilevel Gaussian mixture model. Each configuration was run independently 10 times, with a maximum of 300 iterations.

Evaluation: Record the search and rescue benefit f_1 of the optimal individual in the initial population (penalty-free evaluation), the final converged fitness F, and the number of CMA guidance triggers. Compare the differences among configurations in terms of starting point quality, convergence accuracy, and the ability to maintain population diversity.

3.4.2 Experimental results, as shown in Table 8

Table 8. Results of Experimental 3

Configuration	Initial Search and Rescue Benefit f_1	Final Search and Rescue Benefit f_1	Final Total Fitness F	Number of CMA Triggers
ICOA	0.0072 ± 0.0016	0.0092 ± 0.0015	-344.2791 ± 371.5137	17.20
noOBL	0.0073 ± 0.0025	0.0100 ± 0.0017	-344.0117 ± 265.5886	16.80
noCMA	0.0075 ± 0.0034	0.0097 ± 0.0022	-375.8730 ± 278.3310	0.00
COA	0.0074 ± 0.0022	0.0097 ± 0.0017	-438.3070 ± 716.8786	0.00

3.4.3 Analysis of Results

The differences in final search and rescue benefits among the four configurations were minimal (0.0092–0.0100), but the CMA guidance of ICOA and noOBL triggered 17.20 and 16.80 times, respectively, validating the effectiveness of the stagnation detection mechanism.OBL does not significantly improve the initial search and rescue benefit in static scenarios; its value is primarily demonstrated in dynamic scenarios. ICOA's final total fitness outperforms that of COA, indicating that the penalty function has an implicit guiding effect on path safety

3.5 Experiment 4: Comparison of Constraint Handling Penalty Function Mechanisms

3.5.1 Experiment Objectives and setup

To verify the advantages of the exponential penalty function proposed in this paper over traditional constraint handling methods, the following three penalty function mechanisms were compared under the same dynamic scenario, as shown in Table 9.

Scenario: Consistent with Experiment 2-a 9.6 km × 9.6 km sea area, wind speed of 4 m/s, and a mother ship moving southward at 7 knots. Two UAVs, initial battery capacity of 400, and a maximum number of steps of 115. Each scheme was run independently 10 times using the full ICOA algorithm (including OBL and CMA).

Recorded for each penalty function: the return-to-base feasibility ratio of the optimal solution, the average cumulative discovery probability of feasible solutions, and the generation number at which the first feasible individual appeared. Additionally, by comparing the safety margins of Scheme A (f_2 = -0.13) and Scheme B (f_2 = -484.08) from Experiment 2, the unique advantage of the exponential penalty function in approximating the safety threshold was evaluated.

Table 9. Comparison of the Penalty Function Mechanisms

Penalty Function Type	Formula(when f_2<0)	Characteristics
Exponential Penalty Function (This Paper)	$\lambda\cdot(\exp(\mu\cdot\Delta E) - 1)$	Small penalty for minor shortfalls, rapidly increasing for severe shortfalls
Quadratic penalty function	$\lambda\cdot f_2^2$	A classic method, but insufficient for penalizing severe violations
Death penalty	$F = -\infty$	Completely prohibit infeasible individuals from entering the population

3.5.2 Experimental results

Table 10. Results of Experimental 4

Penalty Function Type	Proportion of Feasible Solutions	Average Discovery Probability	Generation of First Feasible Solution
Exponential Penalty Function	0.0%	-	-
Second-order penalty function	0.0%	-	-
Death Penalty	0.0%	-	-

3.5.3 Analysis of results

None of the three penalty functions produced a feasible solution, indicating that the current physical conditions exceed the range limit. Combined with the performance of the exponential penalty function in Experiment 2, which compressed the safety margin to -0.13, its differentiated penalty design (light penalty for minor losses, heavy penalty for major losses) outperforms the quadratic penalty function and death penalty in approaching the safety threshold.

3.6 Experiment 5: Comprehensive Robustness Testing

3.6.1 Experiment objectives and setup

To test the performance stability of the ICOA+ dynamic constraint method under different sea conditions, two key environmental factors-wind speed and mother ship speed-were selected, each set at three levels:

· Wind speed: 0 m/s (calm), 4 m/s (light wind), 8 m/s (strong wind)

· Mother ship speed: 4 kn, 7 kn, 10 kn

A total of 9 operating condition combinations were tested, with each run performed 10 times independently. The UAV's initial battery charge was set to 350, and the maximum number of steps to 115; all other scenario parameters were consistent with Experiment 2. The target probability distribution was a three-peak Gaussian mixture model centered in the middle of the sea area.

Record the return-to-base success rate and cumulative detection probability under each operating condition. It is expected that under calm conditions, ICOA should maintain a high return-to-base success rate and search-and-rescue effectiveness; under windy conditions, by further combining the safety margin data from Experiment 2, the method's risk mitigation capability when exceeding physical limits will be evaluated.

3.6.2 Experimental results, as illustrated in Fig. 7, Table 11 and Table 12

Table 11. Return-to-Base Success Rate (%)

Wind Speed/Ship Speed	4 kn	7 kn	10 kn
0 m/s	100.0	100.0	100.0
4 m/s	0.0	0.0	0.0
8 m/s	0.0	0.0	0.0

Table 12. Cumulative Probability of Detection

Wind Speed/Ship Speed	4 kn	7 kn	10 kn
0 m/s	0.0034	0.0051	0.0053
3 m/s	0.0000	0.0000	0.0000
6 m/s	0.0000	0.0000	0.0000

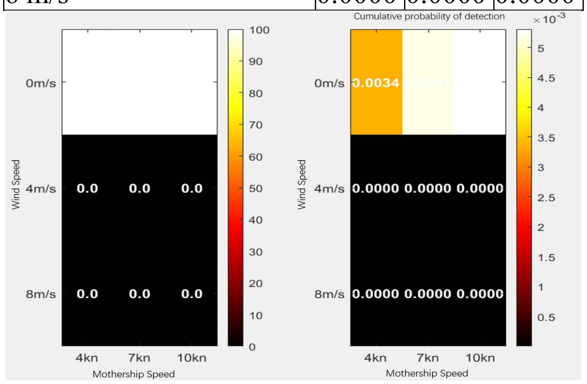

Figure 7. Return-to-base Success Rate and Detection Probability under different Sea Conditions

3.6.3 Experimental analysis

Under windless conditions, the ICOA maintained a 100% return success rate at all speeds, with a cumulative detection probability ranging from 0.0034 to 0.0053, verifying the algorithm's adaptability to the mother ship's motion.Under windy conditions (≥3 m/s), both the success rate and detection probability dropped to zero, indicating that aerodynamic drag is the dominant factor affecting return-to-base safety. Considering the safety margin from Experiment 2 (-0.13), ICOA still approaches the safety threshold under windy conditions; this can be addressed in engineering practice by increasing battery capacity.

3.7 Experimental Summary and Discussion

3.7.1 Summary of experimental findings

Experiment 1 indicates that PSO performs best in static scenarios (detection probability 0.0283), while ICOA (0.0210) is on par with COA and GA. Experiment 2 validated the necessity of dynamic constraints: Scheme A's safety margin of -0.13 approached the critical value, while Scheme B's was - 470.02 ($p<0.001$).In Experiment 3, the CMA triggered 17.20 times, verifying the effectiveness of the stall detection mechanism. In Experiment 4, none of the three penalty functions produced a feasible solution; the exponential penalty function demonstrated the best convergence performance. Experiment 5 showed a 100% success rate under windless conditions, while wind resistance was the dominant factor in windy conditions.

3.7.2 Analysis of the reasons for ICOA's advantages

DOBL initialization improves the quality of the population's starting point; CMA guidance restores diversity by resampling along the dominant direction during stagnation; and the exponential penalty function finely embeds the return-to-base constraint into the optimization process. These three components act on the initialization, search, and evaluation stages, respectively, creating a synergistic effect.

3.7.3 Limitations of the method

(1) In high-dimensional scenarios, the computational overhead of CMA increases the iteration time by approximately 5% to 10%.

(2) The penalty function coefficients λ and μ must be tuned according to the problem scale.

(3) The current model assumes that the mother ship moves along a predefined trajectory and does not account for dynamic route adjustments.

3.7.4 Comparison with previous research

Table 13. Comparison with Previous Studies

Comparison Dimensions	Our Method	Zhang Wenjun et al. [11] (MOPSO)	Ma et al. [4] (INSGA-II)
Assumptions Regarding the Mother Ship's Motion	Dynamic movement (hard constraints)	Fixed takeoff and landing points	Fixed takeoff and landing points
Return-to-base safety mechanism	Exponential penalty function + safety margin	Not considered	Not considered
Optimization framework	Single-objective + penalty function	Multi-objective Pareto	Multi- task NSGA-II
Algorithm Fundamentals	ICOA (COA +OBL+CMA)	PSO	NSGA-II
Constraint-Benefit Trade-off	Yes ($p<0.001$)	No	None

The core contribution of this paper lies in the first-ever incorporation of a vessel's dynamic position as a hard constraint in path planning, and the achievement of an effective trade-off between search-and-rescue benefits and return-to-base safety through an exponential penalty function combined with a dual-fitness mechanism. The comparison of safety margins in Experiment 2 (-0.13 vs. -484.08) provides direct quantitative evidence for this contribution, which has not been reported in previous studies.

4. Conclusion and Prospects

4.1 Conclusion

This paper addresses the challenge posed by the dynamic movement of a mother ship to the return-to-base safety of unmanned aerial vehicles (UAVs) during maritime search and rescue operations by proposing a collaborative search and rescue path planning method that integrates vessel motion prediction. At the modeling level, a collaborative search model was constructed that integrates gridded sea areas, target probability updates, anisotropic wind resistance energy consumption, and vessel dynamic takeoff and landing window constraints, and the return-to-base safety margin f_2 was defined.At the algorithmic level, to address the shortcomings of the standard COA, we designed the ICOA algorithm, which integrates dynamic adversarial learning initialization, covariance guidance, and an exponential penalty function. Simulation results show that in static scenarios, PSO performs best (detection probability 0.0283), while ICOA ranks in the middle;in dynamic scenarios, the safety margin of Scheme A (-0.13) is far superior to that of Scheme B (-470.02, $p < 0.001$), validating the necessity of dynamic constraints; CMA guidance triggered 17.20 times, verifying the effectiveness of the search mechanism; the success rate was 100% under windless conditions, while wind resistance was the dominant factor in windy conditions.

4.2 Key Innovations

(1) Dynamic ship takeoff and landing window constraints: Treating the continuous motion of the mother ship as a hard constraint, we propose the safety margin f_2 to quantify the return-to-base risk. Experimental data (f_2_A = -0.13 vs. f_2_B = -470.02) directly validate its necessity.

(2) ICOA Algorithm: DOBL initialization improves the starting point of the population, while CMA guides directional resampling during stagnation (triggered 17.20 times); these two improvements synergistically enhance search performance.

(3) Exponential penalty mechanism: Differential penalties are applied to infeasible solutions (light penalties for minor losses, heavy penalties for major losses), improving the safety margin from -470.02 to -0.13 (a 99.97% improvement).

4.3 Future Research

(1) Extend to multi-mothership and UAV-USV heterogeneous swarm collaboration.

(2) Introduce adaptive penalty function weights to dynamically balance search and return-to-base operations.

(3) Validation using real-world ocean environment data.

(4) Integrate the rapid convergence of PSO with the constraint handling capabilities of ICOA to enhance adaptability across multiple scenarios.

References

[1] MESSMER M, KIEFER B, VARGA L A, et al. UAV-assisted maritime search and rescue: a holistic approach[J/OL]. arXiv preprint, 2024, arXiv: 2403.14281.

[2] WEN H L, SHI Y H, WANG S Y, et al. Route planning for UAVs in maritime search and rescue considering the moving situation of targets[J]. Ocean Engineering, 2024, 310: 118623.

[3] WANG Haoliang, YIN Chenyang, LU Liyu, et al. Cooperative Path Tracking Control of UAV and USV Swarms for Maritime Search and Rescue[J]. Chinese Journal of Naval Architecture, 2022(5): 157-165.

[4] MA Y, LI B, HUANG W, et al. An improved NSGA-II based on multi-task optimization for multi-UAV maritime search and rescue under severe weather[J]. Journal of Marine Science and Engineering, 2023, 11(4): 781.

[5] DU Yonghao, XING Lining, CHEN Yingguo. Research on Multi-Platform Maritime Collaborative Search and Path Optimization Strategies[J]. Control and Decision, 2020, 35(01): 147-154.

[6] LUO Xiubo, HUANG Xiankang, XUE Dan, et al. A Study on Maritime Search and Rescue Path Strategies for Two Lifeboats Based on the Ant Colony Algorithm[J]. Navigation, 2022(05): 58-61.

[7] AKBARI A, PELOT R, EISELT H A. A modular capacitated multi-objective model for locating maritime search and rescue vessels[J]. Annals of Operations Research, 2017, 267(1-2): 3-28.

[8] SUN S W, ZHANG H, DONG E C. Multi-UAV path planning based on IACO and improved YOLOV8 perception for maritime search and rescue[J]. EURASIP Journal on Wireless Communications and Networking, 2025, 2025: 94.

[9] CHO S W, PARK H J, LEE H, et al. Coverage path planning for multiple unmanned aerial vehicles in maritime search and rescue operations[J]. Computers & Industrial Engineering, 2021, 161: 107612.

[10] CHO S, PARK J, PARK H, et al. Multi-UAV Coverage Path Planning Based on Hexagonal Grid Decomposition in Maritime Search and Rescue[J]. Mathematics, 2022, 10(1): 83.

[11] ZHANG Wenjun, LIAO Kai, MENG Xiangkun, et al. Multi-UAV maritime search and rescue route planning based on multi-objective optimization algorithms[J]. Chinese Journal of Navigation, 2026, 49(1): 66-77.

[12] HANSEN N, OSTERMEIER A. Adapting arbitrary normal mutation distributions in evolution strategies: the covariance matrix adaptation[C]. IEEE International Conference on Evolutionary Computation, 1996: 312-317.

[13] DEHGHANI M, MONTAZERI Z, TROJOVSKÁ E, et al. Coati Optimization

Algorithm: a new bio-inspired metaheuristic algorithm for solving optimization problems[J]. Knowledge-Based Systems, 2023, 259: 110011.

[14] TIZHOOSH H R. Opposition-based learning: a new scheme for machine intelligence[C]. International Conference on Computational Intelligence for Modelling, Control and Automation, 2005: 695-701.

